Locomotion based on Differential Friction

Erik I. Verriest and Deryck Yeung
{erik.verriest,deryck}@ece.gatech.edu
School of Electrical and Computer Engineering
Georgia Institute of Technology
Atlanta, GA 30332, USA

Abstract— This paper analyzes the locomotion of simple mechanisms when the inertial forces are much smaller compared to the applied forces. The induced motion of the body is entirely due to viscous friction contact with the environment. The friction coefficient depends on the body geometry, and we assume a model where it is simply a function of the sign of the velocity. In this case the kinematics and dynamics are easily solvable as a hybrid system. Moreover, scale invariance of the solution is shown. Thus only the pattern as function of time is left to be determined and/or optimized.

We consider a hypothetical flapper in detail, for which the optimal control is derived. This is further illustrated on similar models mimicking locomotion found in nature.

I. INTRODUCTION

Animal locomotion has long been studied by many researchers. Legged locomotion is currently a vast and interdisciplinary field with many contributions from engineers, scientists and applied mathematicians [4]. Unlike legged animals, legless animals such as snakes and fish propel themselves by deforming their body accordingly to interact with the environment. Legless animals are generally more capable in moving on different types of terrains than legged animals. A snake, for example, move effortlessly both on ground and water by using essentially the same type of locomotion. It can also climb trees by extending its body from branch to branch. In comparison, the varieties of legged locomotion seem to be rather small. Swimming is also well studied. For instance, swimming at low speed was studied in [11]. It was shown that at low Reynold's number microscopic organisms propel themselves by periodically changing their body's boundaries. Animal locomotion is the foundation of essentially all biologically inspired robots.

In this paper, inspired by the many varieties of legless locomotion, we shall study self-propulsion of a few legless, toy creatures based on differential friction. This friction model is based on viscous friction which is predominant in wet environment. The model is not as restrictive as it may seem since in [3] it is shown that motion in dry sand can be approximately modeled as motion in fluid. In the differential friction model the friction experienced depends on the direction of locomotion. This results in hybrid systems which are linear in the control. In our study we shall neglect the inertia of the creatures. With this assumption the problem at hand becomes a quasi-static one. This allows us to write down static kinematic equations and static relations between the forces and velocities involved. In [13] this friction

model has been used to study worm-like motion and Fourier techniques have been used to investigate its periodicity.

In section II we introduce the friction model used throughout this paper. In section III we derive the equation of motion of the flapper. In section IV we study the periodic motion of this creature. Several periodic, suboptimal locomotions will be presented. Furthermore, an optimal periodic control will be obtained. In section V we consider several extensions based on the ideas of section III. In section VI we extend the previous results to a simplified model of a snake. In section VII we will conclude and present various future research directions.

II. FRICTION MODEL: DIFFERENTIAL FRICTION

Scales form an integral part of many crawlers. In order to study locomotion effectively the frictional effects of these scales need to be modeled accurately. Scales come in different shapes and sizes. An approximation is shown in Fig.1.
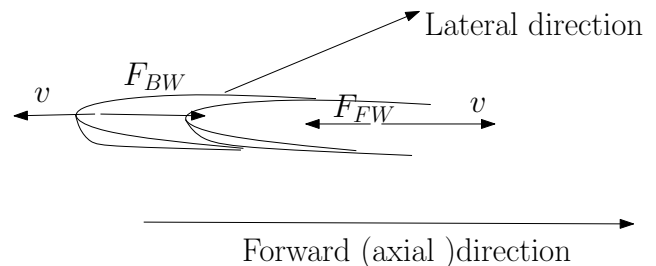

Fig. 1. Differential Friction Model

We model the frictional effects of these scales as the friction one would experience when he/she pushes these rectangular plates raised at one end over a surface. Obviously, the friction experienced depends on the direction in which these plates are being pushed. In short, the differential friction model is a friction model, where the force of friction depends on the direction of locomotion. An animal with scales as in Fig. 1 experiences a friction of $F_{FW} = -\mu_{FW}v$ when the scales slide forward with a velocity v. This friction points to the backwards direction as $\mu_{FW} > 0$ is the *forward* friction coefficient. Similarly, when the scales slide backwards over its environment the total friction is $F_{BW} = -\mu_{BW}v$, where $\mu_{BW} > 0$ is the *backward* friction coefficient. The friction in the transversal or lateral direction is $F_t = -\mu_t v$, where $\mu_t > 0$ is the *transversal* friction

coefficient. In the differential friction model, it is assumed that the friction coefficients satisfy the following ordering: $\mu_{BW} >> \mu_t > \mu_{FW} > 0$, where μ_{BW} is much larger than the other friction coefficients. This implies that the backwards friction F_{BW} is much larger when the scales slide backwards, which agrees with the geometry of the scales of the body. As a shorthand notation, we introduce a function $\mu_A(v)$, which describes the axial friction coefficient with the positive direction shown in Fig. 1. Thus,

$$\mu_a(v) = \begin{cases} \mu_{FW} & \text{if } v > 0; \\ \mu_{BW} & \text{if } v < 0. \end{cases} \quad (1)$$

III. FLAPPER

In this section we consider our first simple toy creature. Consider the flapper system in Fig. 2. Two (inflexible) rods are hinged at O with the scales orientations as shown. We assume that the instantaneous velocity of the flapper aOb is directed towards the left. The half-opening angle is θ. Let $\dot{\theta} = \omega$ be the angular velocity of rod Oa. At a point P, which is a distance s away from the hinge O, the resulting linear velocity is ωs.
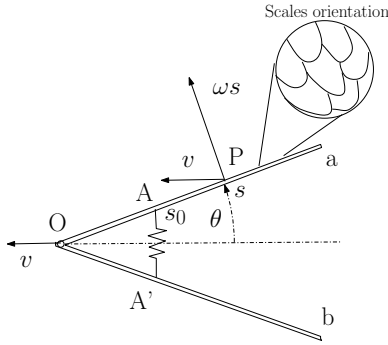

Fig. 2. The Flapper

The combined velocity component in the axial and transversal direction of the section of the rod Oa at P is $v_a = v \cos \theta$ and $v_t = \omega s + v \sin \theta$. This results in an axial and transversal friction force at this point $F_a(s) = -\mu_a(v) v \cos \theta$ and $F_t(s) = -\mu_t (v \sin \theta + \omega s)$. where $\mu_a(v)$ is as defined in (1). We consider F_a positive if directed towards O. Likewise F_t is positive in counterclockwise direction.

Integrating over the total length of Oa, which is assumed to have length one, we get the total axial and transversal force of Oa

$$\mathbf{F}_a = -\mu_a(v) v \cos \theta \quad (2)$$
$$\mathbf{F}_t = -\mu_t \left(v \sin \theta + \frac{\omega}{2} \right). \quad (3)$$

For both rods, the resulting friction forces imposed by v and ω in the x-coordinate direction is

$$\mathbf{F}_x = -\mathbf{F}_a \cos \theta - \mathbf{F}_t \sin \theta \quad (4)$$

and for rod Oa, the resulting friction force in the y-direction is $\mathbf{F}_y = -\mathbf{F}_a \sin \theta + \mathbf{F}_t \cos \theta$. Substituting (2) and (3) into (4) we find the condition for equilibrium: $\mathbf{F}_a \cos \theta + \mathbf{F}_t \sin \theta = 0$ from which $\mu_a(v) v \cos^2 \theta + \mu_t \left(v \sin \theta + \frac{\omega}{2} \right) \sin \theta = 0$. It

follows that for given ω and θ, the instantaneous velocity, neglecting inertia (equivalently, the mass of the flapper is zero), is

$$v(\omega, \theta) = -\frac{1}{2} \frac{\mu_t \omega \sin \theta}{\mu_a(v) \cos^2 \theta + \mu_t \sin^2 \theta} \quad (5)$$

Note that v still appears in the right hand side. However, it is clear that with $\omega > 0$, v must be negative, and vice versa. Hence

$$v(\omega, \theta) = -\frac{1}{2} \frac{\mu_t \omega \sin \theta}{\mu_a(-\omega) \cos^2 \theta + \mu_t \sin^2 \theta} \quad (6)$$

We note that this requires a force $\mathbf{F}$ extended by the arm A'A to counter the vertical friction $\mathbf{F}_y$ $\mathbf{F} = -\mu_a(-\omega) v \cos \theta \sin \theta + \mu_t \left(v \sin \theta + \frac{\omega}{2} \right) \cos \theta$. Substituting the equilibrium condition, we get $\mathbf{F} = \frac{\mu_t \mu_a(-\omega) \omega \cos \theta}{2[\mu_a(-\omega) \cos^2 \theta + \mu_t \sin^2 \theta]}$. The work done by this force when the rod rotates over $\mathrm{d}\theta$ is $\mathrm{d}W = \mathbf{F} \mathrm{d}y = \mathbf{F} s_0 \cos \theta \, \mathrm{d}\theta = \mathbf{F} s_0 \omega \cos \theta \, \mathrm{d}t$. Thus,

$$\mathrm{d}W = \frac{\mu_t \mu_a(-\omega) s_0 \omega^2 \cos^2 \theta}{2[\mu_a(-\omega) \cos^2 \theta + \mu_t \sin^2 \theta]} \, \mathrm{d}t. \quad (7)$$

IV. PERIODIC REGIME

In this section we study the behavior of the flapper when it has a periodic steady state. Equivalently, we may assume that the variables, ω, θ, and v are periodic with period T. We denote the corresponding radial frequency as $\nu = \frac{2\pi}{T}$.

A. Similitude

Assume the applied force is such that it results in an angular velocity $\omega_1(t)$ of the flapper. What happens if we speed this up by a factor k? Let thus $\omega_k(t) = k\omega_1(kt)$. We have $\theta_1(t) = \theta_0 + \int_0^t \omega_1(\tau) \, \mathrm{d}\tau$ and $\theta_k(t) = \theta_0 + \int_0^t \omega_k(\tau) \, \mathrm{d}\tau$. Thus $\theta_k(t) = \theta_0 + k \int_0^t \omega_1(k\tau) \, \mathrm{d}\tau = \theta_0 + \int_0^{kt} \omega_1(\sigma) \, \mathrm{d}\sigma$. and $\theta_k \left(\frac{t}{k} \right) = \theta_0 + \int_0^t \omega_1(\sigma) \, \mathrm{d}\sigma = \theta_1(t)$.

It follows then from (6) also that $v(\omega_k(t), \theta_k(t)) = k \, v(\omega_1(kt), \theta_1(kt))$ Likewise, the rate of applied energy (required instantaneous power) is obtained from (7) and scales as $P(\omega_k(t), \theta_k(t)) = k^2 \, P(\omega_1(kt), \theta_1(kt))$.

The distance traveled by the flapper in one period is given by the integral, assuming k is a positive integer

$$x_k \left(\frac{T}{k} \right) = \int_0^{T/k} v(\omega_k(t), \theta_k(t)) \, \mathrm{d}t = x_1(T). \quad (8)$$

This is therefore independent of the frequency. The energy spent in one complete stroke is

$$\mathcal{E}_k \left(\frac{T}{k} \right) = \int_0^{T/k} P(\omega_k(t), \theta_k(t)) \, \mathrm{d}t = k\mathcal{E}_1(T). \quad (9)$$

Hence to travel a total distance $x_1(T)$, we either spend one cycle at frequency ν, requiring $\mathcal{E}_1(T)$, or k cycles at a frequency $k\nu$. Hence the average velocity is $\overline{v}_k = \frac{x_k(T/k)}{T/k} = \frac{kx_1(T)}{T} = k\overline{v}_1$ and the average power is $\overline{P}_k = \frac{\mathcal{E}_k(T/k)}{T/k} = \frac{k^2 \mathcal{E}_1(T)}{T} = k^2 \overline{P}_1$. This gives a quadratic model for the effective friction. Indeed, consider the simple friction model $F = -\mu_{\text{eff}} v$ A distance x is covered in x/v time units. The

work done against friction is $W = |F|x$. The power is thus $P = |F|x/(x/v) = |F|v = \mu_{\text{eff}} v^2$. Here, we get thus

$$\mu_{\text{eff}} = \frac{\overline{P}_1}{\overline{v}_1^2} = \frac{\mathcal{E}_1/T}{x_1(T)^2/T^2} = T\frac{\mathcal{E}_1(T)}{x_1(T)}. \qquad (10)$$

B. Harmonic control

In this section we do not yet consider the optimal periodic control, but let θ vary harmonically. Let $\theta(t) = \theta_0 + \omega_0 \cos \nu t$ with $\nu = 2\pi/T$. We require that $\theta_0 - \omega_0 \geq 0$ and $\theta_0 + \omega_0 \leq \frac{\pi}{2}$. Then $\omega(t) = -\omega_0 \nu \sin \nu t$, which means that we start with the flapper closing stroke, which provides the push for the creature.

We found for the period $T = 1$ and parameters $\mu_B = 1, \mu_t = 0.5$ the resulting speed (towards the left) and distance traveled in Fig. 3 and Fig. 4 for various values of μ_{FW}, $\mu_{FW} = 0.01, 0.1$ and 1. As expected, in the latter case there is no net motion and the most power is consumed. The required power as function of the time within one period is also shown for the same values of μ_{FW} in Fig. 5.

The effective friction coefficient for the flapper is shown as function of μ_{FW} for this periodic regime with $\mu_t = 0.5$ and $\mu_{BW} = 1$ in Fig. 6.
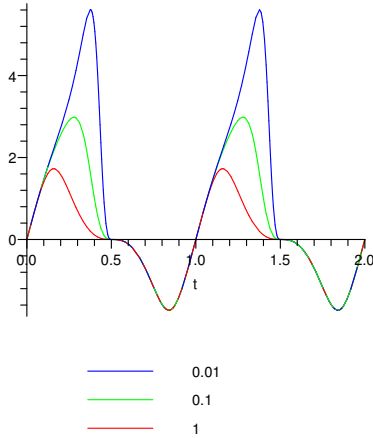

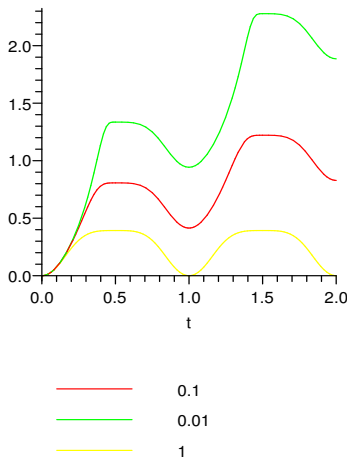Fig. 3. Speed for $\mu_{FW} = 0.01, 0.1, 1, \mu_B = 1$ and $\mu_t = 0.5$.

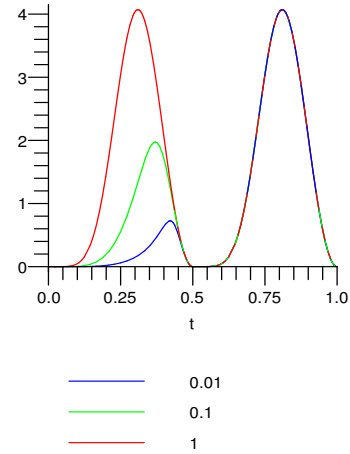Fig. 4. Distance traveled for $\mu_{FW} = 0.01, 0.1, 1, \mu_B = 1$ and $\mu_t = 0.5$.

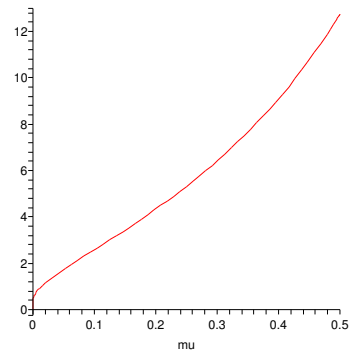Fig. 5. Power for $\mu_{FW} = 0.01, 0.1, 1, \mu_B = 1$ and $\mu_t = 0.5$.

Fig. 6. Effective friction coefficient.

C. Optimal Periodic Regime

In this section we will study the optimal periodic control. Assume that the flapper's motion is in a periodic steady state with period T. Over one period the excursion of the flapper is $x(T) = \int_0^T v(\omega, \theta)\, dt$. We maximize the excursion in one period with the constraints that the amount of energy is fixed, i.e $W(T) = W_T$ and that the motion is periodic; $\theta(0) = \theta_0 = \theta(T)$. Let θ_0 be arbitrary in $[0, \pi/2]$. The extended state equations are $\dot{\theta} = \omega$, $\dot{W} = \frac{\mu_t \mu(-\omega) s_0 \omega^2 \cos^2 \theta}{2[\mu_a(-\omega)\cos^2 \theta + \mu_t \sin^2 \theta]}$. The control input is ω. From (6) the Hamiltonian is

$$H = \frac{1}{2}\frac{\mu_t \omega \sin \theta}{\mu_a(-\omega)\cos^2 \theta + \mu_t \sin^2 \theta} + \lambda_\theta \omega + \\ + \lambda_W \frac{\mu_t \mu_a(-\omega) s_0 \omega^2 \cos^2 \theta}{2[\mu_a(-\omega)\cos^2 \theta + \mu_t \sin^2 \theta]}$$

Since the function $\mu_a(-\omega)$ is not differentiable the Pontryagin Maximum Principle [6] needs to be used. The Hamiltonian is bi-modal and it is quadratic in ω for $\omega > 0$ and $\omega < 0$. Therefore, the optimality condition for $\omega > 0$, the backward moving stroke, is $\omega_{BW} = \frac{-\mu_t \sin \theta - 2\lambda_\theta[\mu_{BW}\cos^2 \theta + \mu_t \sin^2 \theta]}{2\lambda_W \mu_t \mu_{BW} s_0 \cos^2 \theta} > 0$. For $w < 0$, the forward moving stroke, is $\omega_{FW} = \frac{-\mu_t \sin \theta - 2\lambda_\theta[\mu_{FW}\cos^2 \theta + \mu_t \sin^2 \theta]}{2\lambda_W \mu_t \mu_{FW} s_0 \cos^2 \theta} < 0$, The costate equations are $\dot{\lambda}_\theta = -\frac{\partial H}{\partial \theta}$ and $\dot{\lambda}_W = -\frac{\partial H}{\partial W} = 0$.

For the simulation it is assumed that the period $T = 1$sec and the initial starting angle $\theta(0) = \pi/17$. A standard gradient descent algorithm has been implemented to find the optimal control $\omega(t)$. The results are shown in Fig. 7, Fig. 8, Fig. 9 and Fig. 10. As in Fig. 10 the creature goes backwards initially when opening its flappers and moves forward when they are closed. The net effect is a forward motion due to the differential friction.
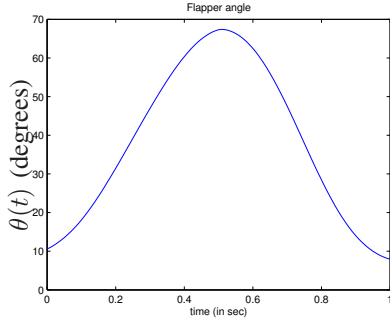

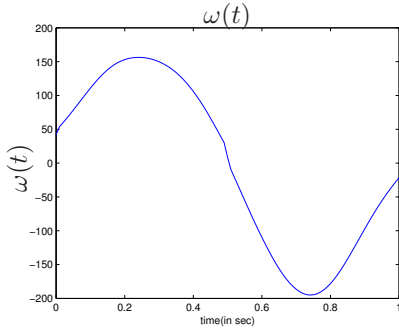Fig. 7.   Flapper's angle $\theta(t)$
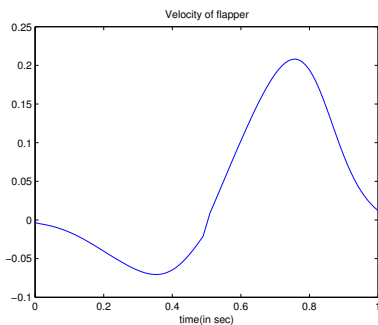

Fig. 8.   Angular frequency $\omega(t)$

Fig. 9.   Velocity $v(t)$

V. EXTENSIONS

Previous discussions can be extended to other robotic devices. One could offset two flappers to obtain a tortoise Fig. 11. In this case the flapper angles θ_1 and θ_2 have
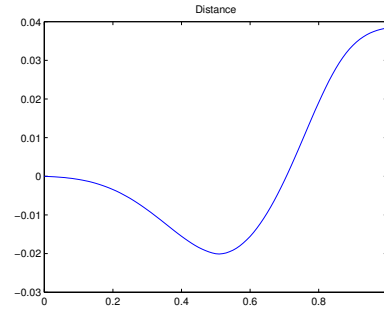

Fig. 10.   Distance $x(t)$

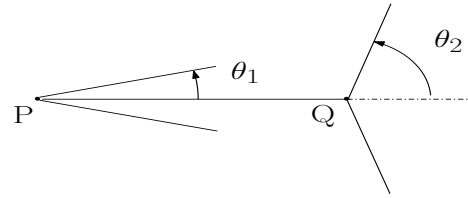opposite phases to accommodate locomotion. In the next section we will extend the flapper to a simplified snake model.

Fig. 11.   Tortoise

VI. TWO-PIECE SNAKE

We extend the previous analysis to a simplified model of a snake, Fig. 12. We will derive the friction forces exerted by the environment on the snake. First, consider a small piece with length dr of the snake from either the upper or lower bar, which is located at $r(t)$ with respect to a inertial reference frame with basis $\{e_x, e_y\}$, Fig. 13.

According to the differential friction model (1) the friction experienced by this differential slab is

$$
\begin{aligned}
F_{B_x}(r, \beta) &= -\mu_a(\langle \dot{r}, B_x \rangle)\langle \dot{r}, B_x \rangle B_x \\
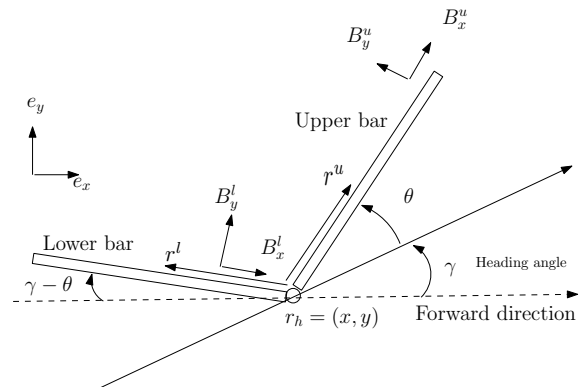F_{B_y}(r, \beta) &= -\mu_T \langle \dot{r}, B_y \rangle B_y,
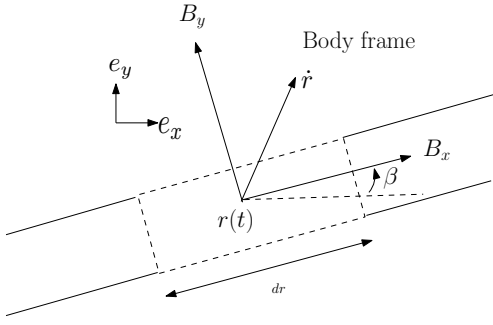\end{aligned} \tag{11}
$$

Fig. 12.   Two-piece snake.

Fig. 13. Differential piece of snake.

where $\langle \cdot, \cdot \rangle$ denotes the inner product, $B_x = \begin{bmatrix} \cos(\beta) & \sin(\beta) \end{bmatrix}'$ is the axial direction and $B_y = \begin{bmatrix} -\sin(\beta) & \cos(\beta) \end{bmatrix}'$ is the transversal direction, both with respect to the inertial reference frame. The total x and y components of the friction force are $F_x(r, \beta) = \langle F_{B_x}, e_x \rangle + \langle F_{B_y}, e_x \rangle$, and $F_y(r, \beta) = \langle F_{B_x}, e_y \rangle + \langle F_{B_y}, e_y \rangle$, respectively. The virtual work due to virtual displacements in the x and y direction of the differential piece at r is

$$\delta W_r = F_x(r, \beta)\delta x + F_y(r, \beta)\delta y \qquad (12)$$

We now proceed to derive the friction forces acting on the entire snake. Let $r_h = (x, y)$ denote the position of the hinge of the snake, Fig. 12. We further assume that both links have unit length. A point $r \in [0, 1]$ units away from the hinge on the upper and lower bar is

$$r^u = r_h + rB_x^u, \qquad (13)$$
$$r^l = r_h - rB_x^l, \qquad (14)$$

where with respect to the inertial reference frame, $B_x^u = \begin{bmatrix} \cos(\theta + \gamma), & \sin(\theta + \gamma) \end{bmatrix}'$ and $B_x^l = \begin{bmatrix} \cos(\gamma - \theta), & \sin(\gamma - \theta) \end{bmatrix}'$, respectively. We will use the Lagrangian dynamics approach to find the generalized friction forces. Recall the Euler-Lagrange equations

$$\frac{d}{dt}\frac{\partial L}{\partial \dot{q}} - \frac{\partial L}{\partial q} = Q, \qquad (15)$$

where L is the Lagrangian and Q contains the external and control forces. Let the generalized coordinates be $q = [x, y, \theta, \gamma]$, Fig. 12. From (13) the virtual displacements at a distance r from the hinge on the *upper* bar, $\delta r^u = (\delta x_r^u, \delta y_r^u)$, due to the virtual displacements in the generalized coordinates, are

$$\delta x_r^u = \delta x - r\sin(\theta + \gamma)(\delta\theta + \delta\gamma), \qquad (16)$$
$$\delta y_r^u = \delta y + r\cos(\theta + \gamma)(\delta\theta + \delta\gamma)$$

Similarly from (14), the virtual displacements on the *lower* bar are

$$\delta x_r^l = \delta x + r\sin(\gamma - \theta)(\delta\gamma - \delta\theta), \qquad (17)$$
$$\delta y_r^l = \delta y - r\cos(\gamma - \theta)(\delta\gamma - \delta\theta)$$

Substituting $(13), (14), (16), (17)$ into (12), the friction forces on both the upper and lower bar r units away from the hinge r_h may be expressed in the form

$$\delta W_r = T_x(r, \dot{x}, \dot{y}, q)\delta x + T_y(r, \dot{x}, \dot{y}, q)\delta y + $$
$$+ T_\theta(r, \dot{x}, \dot{y}, q)\delta\theta + T_\gamma(r, \dot{x}, \dot{y}, q)\delta\gamma. \quad (18)$$

The exact expressions are omitted due to the limitation of space.

Integrating the previous expression (18) over $[0, 1]$, we obtain the total virtual work of the external friction forces on the *entire* snake. Indeed, the integral is

$$\delta W = \underbrace{\int_0^1 T_x(r, \dot{x}, \dot{y}, q)dr}_{F_x^t(\dot{x}, \dot{y}, q)} \delta x + \underbrace{\int_0^1 T_y(r, \dot{x}, \dot{y}, q)dr}_{F_y^t(\dot{x}, \dot{y}, q)} \delta y$$
$$+ \underbrace{\int_0^1 T_\theta(r, \dot{x}, \dot{y}, q)dr}_{F_\theta^t(\dot{x}, \dot{y}, q)} \delta\theta + \underbrace{\int_0^1 T_\gamma(r, \dot{x}, \dot{y}, q)dr}_{F_\gamma^t(\dot{x}, \dot{y}, q)} \delta\gamma,$$

from which we can easily identify the total generalized friction forces, $F_x^t(\dot{x}, \dot{y}, q), F_y^t(\dot{x}, \dot{y}, q), F_\theta^t(\dot{x}, \dot{y}, q)$ and $F_\gamma^t(\dot{x}, \dot{y}, q)$.

The applied control is the torque F_c around the hinge. The external generalized force Q in (15) is

$$Q = [F_x^t(\dot{x}, \dot{y}, q), F_y^t(\dot{x}, \dot{y}, q), F_\theta^t(\dot{x}, \dot{y}, q) + F_c, F_\gamma^t(\dot{x}, \dot{y}, q)]' (19)$$

We further assume that the snake is in a quasi-periodic state and the inertia is small. This allows us to set the left hand side of (15) to zero, because the Lagrangian is linear in mass. Then (19) can be rewritten in the form

$$A(\dot{x}, \dot{y}, q)\dot{q} = [0, 0, F_c, 0]'. \qquad (20)$$

After a long but straight forward computation, the determinant of $A(\dot{x}, \dot{y}, q)$ can be shown to be

$$\det A(\dot{x}, \dot{y}, q) = a\cos(\theta)^4 - a\cos(\theta)^2 + \frac{2\mu_T^2}{9}(g_u + g_l), (21)$$

where

$$g_u = \mu_a(\langle \dot{r}^u, B_x^u \rangle) = \mu_a(\dot{x}\cos(\theta + \gamma) + \dot{y}\sin(\theta + \gamma)) \quad (22)$$
$$g_l = \mu_a(\langle \dot{r}^l, B_x^l \rangle) = \mu_a(\dot{x}\cos(-\theta + \gamma) - \dot{y}\sin(-\theta + \gamma))$$

and $a = -\frac{\mu_T^2}{9}(\mu_T^2 - 4(g_u + g_l)\mu_T + 16g_u g_l)$. It is obvious that, since $-\frac{\pi}{2} \leq \theta \leq \frac{\pi}{2}$, (21) is quadratic in $\cos(\theta)^2$ over the interval $[0, 1]$. The extremum of (21) is at $\cos(\theta)^2 = 1/2$ and at this value (21) is $\frac{\mu_T^2}{36}(\mu_T^2 + 4(g_l + g_u) + 16g_l g_u) > 0$ by the positivity of each term. Furthermore, if $\cos^2\theta = 0$ or 1 (i.e., $\theta = \pm\frac{\pi}{2}$ or $\theta = 0$), then (21) is $\frac{2\mu_T^2}{9}(g_u + g_l) > 0$ by the definition of $\mu_a(\cdot)$. Thus, (21) is always positive in the interval $-\frac{\pi}{2} \leq \theta \leq \frac{\pi}{2}$, regardless of the sign of a. Thus $A(\dot{x}, \dot{y}, q)$ is invertible over th interval. Hence, (20) can be written

$$\dot{q} = \frac{b(\dot{x}, \dot{y}, q)}{\det A(\dot{x}, \dot{y}, q)}F_c, \qquad (23)$$

where $b(\dot{x}, \dot{y}, q)$ is the third column of the adjugate matrix, Adj $A(\dot{x}, \dot{y}, q)$.

Due to the bi-modal nature of $\mu_a(\cdot)$ the system (23) is hybrid and from the previous equations it seems that the system has at least 4 modes. However, it can shown that

$$\frac{\langle \dot{r}^u, B_x^u \rangle}{\langle \dot{r}^l, B_x^l \rangle} = -\frac{4g_l + \mu_T \tan^2 \theta}{4g_u + \mu_T \tan^2 \theta}, \qquad (24)$$

by using the first two components of (23). Thus, the velocities on both the upper and lower link along the axial directions, at a distance r away from the hinge, have opposite sign. This further implies that when the upper link is gliding forward, the lower link is sliding backwards and vice versa.

We now proceed to compute the work imparted by the snake. From (11) the total friction forces *on* the snake at both the upper and lower link, at a distance r from the hinge r_h, are $F_{tot}^u(r) = F_{B_x}(r^u, \theta + \gamma) + F_{B_y}(r^u, \theta + \gamma)$ and $F_{tot}^l(r) = F_{B_x}(r^l, -\theta + \gamma) + F_{B_y}(r^l, -\theta + \gamma)$, respectively. The total work at r is

$$W_{tot}(r) = F_{tot}^u(r) \frac{dr^h}{dt} dt + F_{tot}^l(r) \frac{dr^l}{dt} dt.$$

After dividing the previous expression by dt and integrating over $[0, 1]$, we obtain the power consumed *by* the snake is

$$\frac{dW_{tot}}{dt} = -\left(\int_0^1 F_{tot}^u(r) \frac{dr^h}{dt} dr \right) - \left(\int_0^1 F_{tot}^l(r) \frac{dr^l}{dr} \right). \quad (25)$$

To simulate the snake we assume the input torque is $F_c(t) = 20 \cos t$. The starting angles are $\theta(0) = 0$ and $\gamma(0) = -0.35$. The simulation duration is over one period $T = 2\pi$. (Fig. 14). The forward direction is to the right. As in the flapper the two-piece snake slides backwards initially and then forward. The locomotion is inefficient as seen in the figure. The total distance traveled sideways is almost four times the forward motion. This is due to the overly simplified model. If additional links are added, this sideways motion will decrease substantially. Notice that when the torque is positive (counter clockwise) the snake moves in the negative y-direction, and vice verse for clockwise torque. This is in accordance with our intuition because of the tangential (to the body) friction. It is also shown by experimentation that sideways motion is decreased when the tangential coefficient μ_T is increased (for rounded scales).
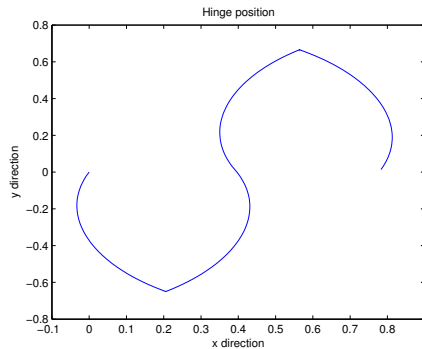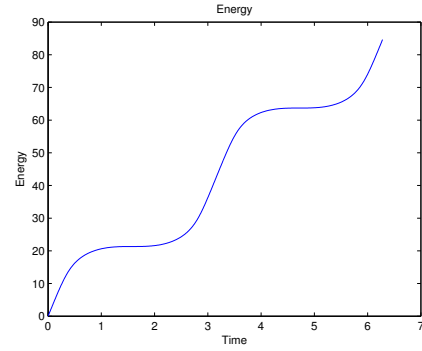

Fig. 15. Energy expended snake .

VII. Conclusions

In this paper we introduced the differential friction model which was used throughout the paper to study locomotion. As a result of this model the equations of motions obtained are of hybrid nature which are linear in the control. In our study we have neglected inertia of the creatures considered. This allowed us to obtain static relations between the forces and velocities for our creatures. This is not particularly restrictive since it is long known that acceleration is only a means to an end when it comes to locomotion [1]. Furthermore, we have studied the locomotive behavior under periodic steady state assumption. Suboptimal periodic controls as well as an optimal periodic control problem were considered.

References

[1] Childress, S., *Mechanics of Swimming and Flying*, Cambridge University Press, 1981.

[2] Earhart, G.M. and P.S.G. Stein, "Step, Swim and Scratch Motor Patterns in the Turtle," *J. Neurophysiol,* Vol **84**, pp. 2181-2190, 2000.

[3] Zhu, Y. *Animating Sand as a Fluid,*, M.Sc thesis, University of Britisch Columbia, 2005.

[4] Holmes, P., R.J. Full, D. Koditschek, and J. Guckenheimer, "The Dynamics of Legged Locomotion: Models, Analyses, and Challenges," *SIAM Review* Vol. 48, No. 2, pp. 207-304.

[5] Alexander, R.McNeill, *Principles of Animal Locomotion*, Princeton University Press, 2003.

[6] A.E. Bryson and Y.C. Ho, *Applied Optimal Control*, Hemisphere Publishing Corporation 1975.

[7] J.H Long Jr, J.Schumacher, N. Livingston and M. Kemp, " Four flippers or two? Tetrapedal swimming with an aquatic robot" *Bioinspiration & Biommimetics 1* , 2006, pp. 20-29.

[8] Hirose, S., *Biologically Inspired Robots: Snake-like Locomotors and Manipulators*, Oxford Univ. Press, Oxford, 1993.

[9] Persson, B.N.J., *Sliding Friction*, Second Edition, Springer-Verlag, 2000.

[10] Chernousko, F.L., "Snake-Like Motions of Multibody Systems over a Rough Plane," *Proc. COC*, Vol. 2, St Petersburg, Russia, pp. 321-326, 2000.

[11] Shapere, A. and F. Wilczek, "Self-Propulsion at Low Reynolds Number," *Physical Review Letters*, Vol. 58, No. 20, pp. 2051-2054, May 1987.

[12] Verriest, E.I., "Efficient Motion Planning for a Planar Multiple Link Robot, Based on Differential Friction," *Proceedings of the 1989 American Control Conference*, Pittsburgh, Pennsylvania, pp. 2364-2365, June 1989.

[13] Verriest, E.I. "Locomotion of Friction Coupled Systems," the IFAC Workshop on Periodic Systems Control (PSYCO-07), St-Petersburg, Russia, August 2007.

Fig. 14. Hinge position $r_h(t)$.